

Intermolecular Coulombic decay by concerted transfer of energy from photoreceptors to a reaction center

Saroj Barik,¹ Nihar Ranjan Behera,¹ Saurav Dutta,¹ Y. Sajeev,^{2, a)} and G. Aravind^{1, b)}

¹⁾*Department of Physics, Indian Institute of Technology Madras, Chennai, India*

²⁾*Theoretical Chemistry Section, Bhabha Atomic Research Centre, Mumbai, India*

(Dated: 21 June 2023)

Molecular mechanisms that enable concerted transfer of energy from several photoacceptors to a distinct reaction center are most desirable for the utilization of light-energy. Here we show that intermolecular Coulombic decay, a channel which enables non-local disposal of energy in photoexcited molecules, offers an avenue for such a novel energy-transfer mechanism. On irradiation of pyridine-argon gas mixture at 266 nm and at low laser intensities, we observed a surprisingly dominant formation of argon cations. Our measurements on the laser-power dependence of the yield of the Ar cations reveal that intermolecular Coulombic interactions concertedly localize the excitation energy of several photoexcited pyridines at the argon reaction center and ionize it. The density of the reaction center offers an efficient handle to optimize this concerted energy-transfer. This mechanism paves the way for a new π -molecular light-harvesting system, and can also contribute to biomolecular stability against photodamage.

I. INTRODUCTION

Intermolecular Coulombic decay (ICD) is the most efficient and ubiquitous relaxation pathway by which excited molecules in a molecular environment relax by ionizing their neighbours¹⁻⁵. Following the theoretical prediction of ICD¹, a number of experiments revealed this relaxation channel in several molecular environments⁴⁻¹⁸. Due to the strong dependence of the ICD rates on the intermolecular interactions, early reports on its measurements were essentially on rare gas clusters. While ICD has also been reported in many natural molecular systems, including liquid water¹⁹, π -stacked aromatic molecules²⁰, and hydrogen-bonded dimers, they all are mainly concerned with the electronic relaxation of an inner-valence ionized state created by ionizing radiation or electron impact. A recently reported experiment in which π -molecules collectively relax via a highly efficient multi-center ICD, following their $\pi - \pi^*$ photoexcitation at ambient UV intensity, demonstrates that this mechanism is also of great importance in general photochemistry³¹. The efficiency of this multi-center mechanism is revealed by the fact that the ICD operates through an associative covalent interaction even when the π -molecules are unbound in their ground state. It is, therefore, apparent that this multi-center ICD mechanism is a fundamental reaction channel to explore for the nonlocal utilization of excitation energy in π -molecular systems.

The nonlocal and simultaneous utilization of excitation energy, by its transfer from several photoexcited π -molecules to a distinct non-photoabsorbing reaction center, is not known but is most desirable in many fields of science. DNA and light-harvesting (LH) systems are two examples where many π molecules can undergo simultaneous photoexcitation. DNA, made up of π -electron nucleobases, is one of the macromolecules susceptible to UV induced direct damage²². When multiple nucleobase moieties of DNA absorb UV radiation, a deposition in excess of 3 eV on each of the bases can trigger a variety of photochemical reactions in the DNA leading to mutagenesis and carcinogenesis^{7,23-25}. Ultrafast and nonlocal disposal of

^{a)}Electronic mail: sajeevy@barc.gov.in

^{b)}Electronic mail: garavind@iitm.ac.in

this excess electronic energy accumulated on adjacent bases is the key to prevent its photo-damage. Therefore, the possibility that excited nucleobases can use their excitation energy to ionize the DNA counter-ion and thereby relax collectively warrants a discussion. Similarly, given the fact that many receptors are simultaneously photoexcited in a π -molecular LH system, the availability of nonlocal molecular mechanisms that help to control the rapid and concerted flow of electronic energy from several receptors to a reaction center can be considered a major challenge for the development of future LH systems.

As a relaxation channel facilitating nonlocal transfer of electronic energy from photoexcited molecules, the ICD mechanism is an obvious solution to the two challenges discussed above. But, although ICD mechanisms involving energy transfer between photoexcited molecules and, between a photoexcited molecule and its neighbour, have been reported, there is a void in our knowledge on ICD mechanisms that involve concerted and efficient transfer of electronic energy from several photoexcited molecules to a distinct non-photoabsorbing reaction center. Therefore, by keeping these two challenges in focus, to study concerted transfer of electronic energy within an unbound environment consisting of photoreceptors and reaction centers, we explore here an ICD that ensues photoabsorption in an unbound system of pyridine monomers diluted in argon (Ar) gas.

II. RESULTS AND DISCUSSION

The pyridine-argon molecular environment was irradiated with 266 nm photon beam. Even at low laser intensities between $10^4 - 10^6$ Wcm⁻², we observed a surprisingly dominant formation of argon cations, as shown in Figure 1. All the cations that were observed in the undiluted pyridine experiments³¹ were also observed. Velocity map image (VMI) of the electrons emitted in the present experiment, i.e., on irradiation of the pyridine-argon environment, is shown in Figure 5. The VMI shows isotropic emission of electrons with kinetic energies ranging between 0-0.6 eV.

We now consider the formation of Ar⁺ cations in our experiments. The single-photon energy (4.661 eV) is way below the ionization threshold of Ar (15.75 eV). Thus, four-photon energy is required for ionizing the Ar atoms. The laser-intensities employed here are low for the occurrence of multi-photon ionization (MPI) in argon. There are no resonant transitions in argon at 266 nm which could enhance the MPI. Further, since four photons are required for the MPI of argon, the plot for $\log(\text{Ar}^+ \text{ yield})$ vs $\log(\text{laser-pulse intensity})$ should have a value of 4 for its slope. However, in the present experiments, the value for this slope is nearly 1, as shown in Figure 1. The observed isotropic emission of electrons from argon atoms is also not expected in a MPI process. Thus, the linear variation of the yield of Ar⁺ cations with the laser power and the isotropic emission of electrons unambiguously rule out the photoionization of argon atoms in our experiments. Therefore, considering the fact that pyridine undergoes $\pi - \pi^*$ resonant excitation at 266 nm, the observation of dominant Ar⁺ cations in Ar-pyridine gas mixture, at ambient intensity of this light, is a key to explore the mechanism of concerted transfer of electronic energy from multiple photoacceptors to a reaction center.

Three important experimental observations shed light on the mechanism behind the observed formation of Ar⁺ cations. First, Ar⁺ cations are formed under experimental conditions where pyridine monomers are dissolved in Ar gas. However, under the same laser-beam conditions, Ar⁺ cations are not formed when Ar gas alone is used. Second, as mentioned above, despite the requirement of four-photon energy, the laser-power dependence for the yield of Ar⁺ cations is linear. These two features affirm a resonant single-photon absorption in pyridine molecules followed by a non-local transfer of electronic energy from π^* -excited pyridine molecules to Ar atoms. Since the non-local transfer of electronic energy depends only on the electron-electron correlations, the overall laser-power dependence for the yield of Ar⁺ cations will be that of the preceding step *viz.* single-photon absorption^{2,10}. Hence, this linear laser-power dependence for the yield of Ar⁺ cations affirms ICD ionization of the Ar atoms. Lastly, the observation of isotropic emission of electrons is characteristic of ICD

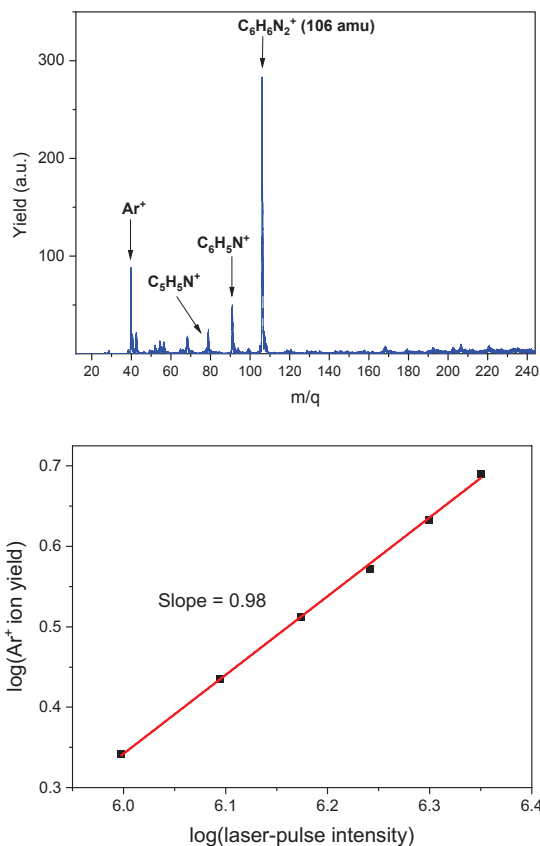


FIG. 1. Time-of-flight mass spectrum of cations and the laser-power dependence for Ar^+ yield: The mass spectrum in the top panel shows the dominant formation of argon cations and other cations from pyridine upon irradiation of pyridine-Ar gas mixture. For this measurement, pyridine at its vapour pressure was diluted with 1 atm. of Ar gas. The laser wavelength employed was 266 nm at an intensity of $2.4 \times 10^6 \text{ Wcm}^{-2}$. Adjacent-averaging of the raw data points was performed using Origin 7.5 software for this plot. The laser power dependence of the Ar^+ yield is linear as shown in the bottom panel. a.u., arbitrary units.

ionization. In this experiment, the ICD ionization is a Coulombic decay involving concerted transfer of electronic energy from four photoexcited pyridine molecules to an Ar atom.

We now discuss the Coulombic decay in photoexcited pyridine molecules that leads to the formation of Ar^+ cations under our experimental conditions. The π -electron molecules exhibit long-range associative covalent interactions in their π^* excited state. Therefore, under our experimental conditions, the dominant ICD channels are expected to originate through the dimers of excited state pyridines, which are formed by this interaction. The two-photon energy in such dimers is barely above the ionization potential of pyridine and hence the intramolecular vibrational energy redistribution (IVR) would render the two-photon energy off-resonant for ionization in pyridine dimers³¹. Hence, such a dimer of excited pyridines can primarily relax through an ICD channel by its direct interactions with an excited monomer or with another dimer of excited pyridines. This direct ICD channel is very efficient because it is driven by covalent interactions between the π^* -excited states of the pyridine units³¹. The insertion of argon atoms into this photoexcited pyridine system opens a new competitive ICD channel involving the argon atom and two dimers of excited pyridines. Since the relative yield of the argon cation is observed to be significant and competing with the direct ICD products involving only photoexcited pyridine units, this channel must also be driven by efficient covalent interactions between the participating

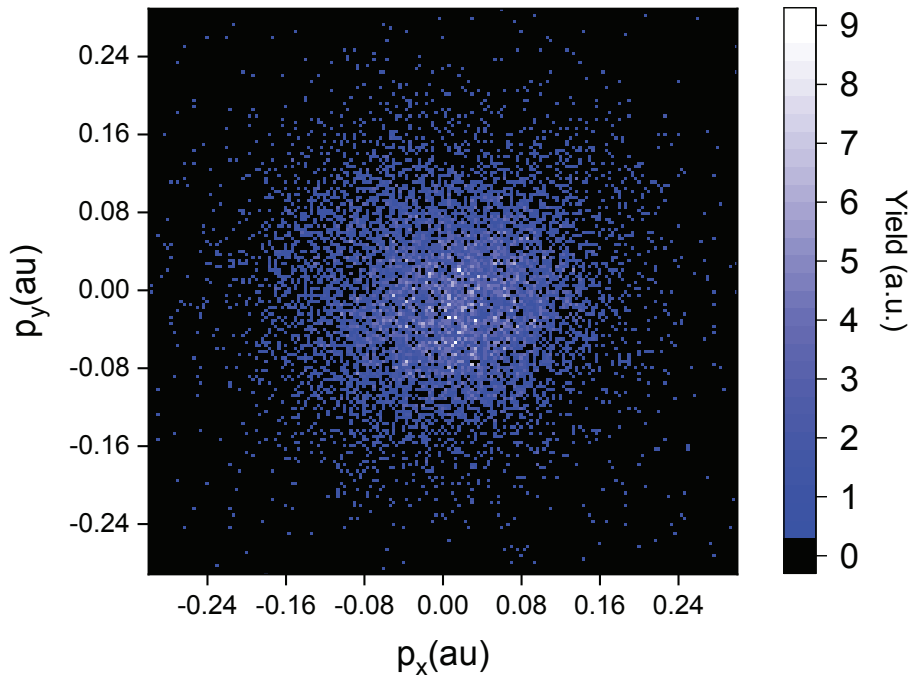


FIG. 2. **VMI of ICD electrons:** VMI showing isotropic emission of ICD electrons from Ar atoms and pyridine molecules, where the imaging is not done in coincidence with any particular cation. au, atomic units.

units, *i.e.*, two dimers of excited pyridines and an argon atom. To understand the extent of the covalent interaction between the argon atom and the two dimers, we calculated the electron density distribution of the molecular units that comprise them (see the *Methods* section for computational details).

On the basis of our experimental observation and quantum chemical calculations, a molecular mechanism for the ionization of an argon atom via ICD due to its interaction with two dimer units of excited-state pyridines is shown in Figure 3. When an argon atom diffuses into the noninteracting interior space of two dimers of photoexcited pyridines, the intermolecular covalent interaction between the dimers is activated by the Ar atom. As a result, the ICD is activated and the molecular system relaxes by ionizing the Ar atom. A covalent mixing of 1π orbitals of pyridines with the $3p_z$ atomic orbital of the argon atom is responsible for the concerted relaxation of energy via the ICD channel. This covalent mixing of orbitals is seen even when Ar and excited pyridines are separated by more than 10\AA .

As mentioned earlier, a doubly-excited pyridine dimer could associate with a photoexcited dimer or a monomer and undergo ICD. The electronic energy transfer from the doubly excited dimers to argon atoms should compete with the above mentioned ICD that occurs between photoexcited pyridine units. At higher laser intensities, when the number density of photoexcited dimers increases, the ICD between the photoexcited pyridine units would increasingly dominate over the ionization of Ar. At lower number densities of photoexcited dimers, the separations between them being larger, the probability for ionizing Ar atoms *en route* to their association increases. Hence, the ratio of the yield of Ar^+ cation to that of the total yield of all the other cations originating from photoexcited pyridines should increase with decreasing laser intensities, and this is observed in our experiments, as shown in Figure 4. Further, the relative yield of argon cations were observed to also increase with increasing partial pressure of the argon gas, as shown in Figure 4. These two observations unequivocally assert the concerted ICD mechanism between several photoreceptors and a distinct reaction center. Increasing relative yield of Ar^+ cations implies efficient energy transfer. Hence, it is seen that both the laser intensity and the partial pressure of the argon

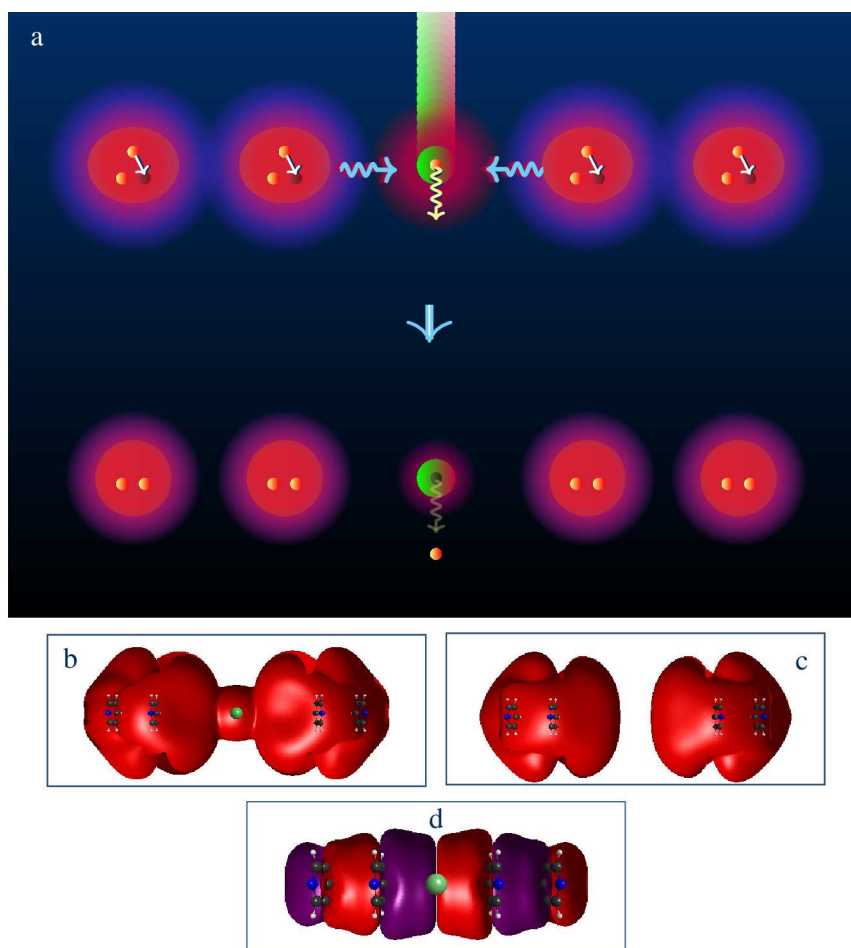


FIG. 3. **Molecular mechanism of photoexcited pyridine molecules ionizing an argon neighbor via ICD:** **a**, Argon atom is shown in green while pyridine is shown in red. The haze represents the valence electron density, and the blue outer haze represents the photoexcited electron density of pyridine. Intermolecular covalent interactions between two non-interacting dimers of photoexcited pyridines are activated by the diffusion of an Ar atom into the noninteracting inter dimer space. Consequently, the ICD becomes operative, and ionizes the Ar atom. **b-c**, The overlap of the wavefunction due to diffusion of the Ar atom into the non-interacting inner dimer space is shown by comparison of the total electron density surfaces with and without the argon atom, where the surfaces are plotted for a very small iso-density value of 1×10^{-6} . **d**, The intermolecular orbital formed from the covalent mixing of 1π orbitals of pyridines with the $3p_z$ orbital of the argon atom is shown, where a 4\AA of pyridine-argon separation is used for better visualization of the covalent mixing.

reaction center offer an efficient handle to optimize this concerted energy transfer.

A few important remarks on the generality of this concerted ICD mechanism is in order. The ionization of the argon atom serves here as a model for the reaction that would occur due to the concerted energy-transfer from several excited pyridine centers to a distinct reaction center. Any reaction occurring at the reaction center due to the availability of electronic energy, by concerted localization of excitation energy in general, but not limited to such hole-particle separation, can be initiated through this mechanism. Moreover, since the mechanism is initiated due to the overlap of wavefunctions, this concerted transfer of energy to the reaction center may originate not only from a collection of $\pi - \pi^*$ excited states, but also from a set of $n - \pi^*$ states or molecular Rydberg states.

To conclude, our measurements on the laser-power dependence for the yield of Ar cations,

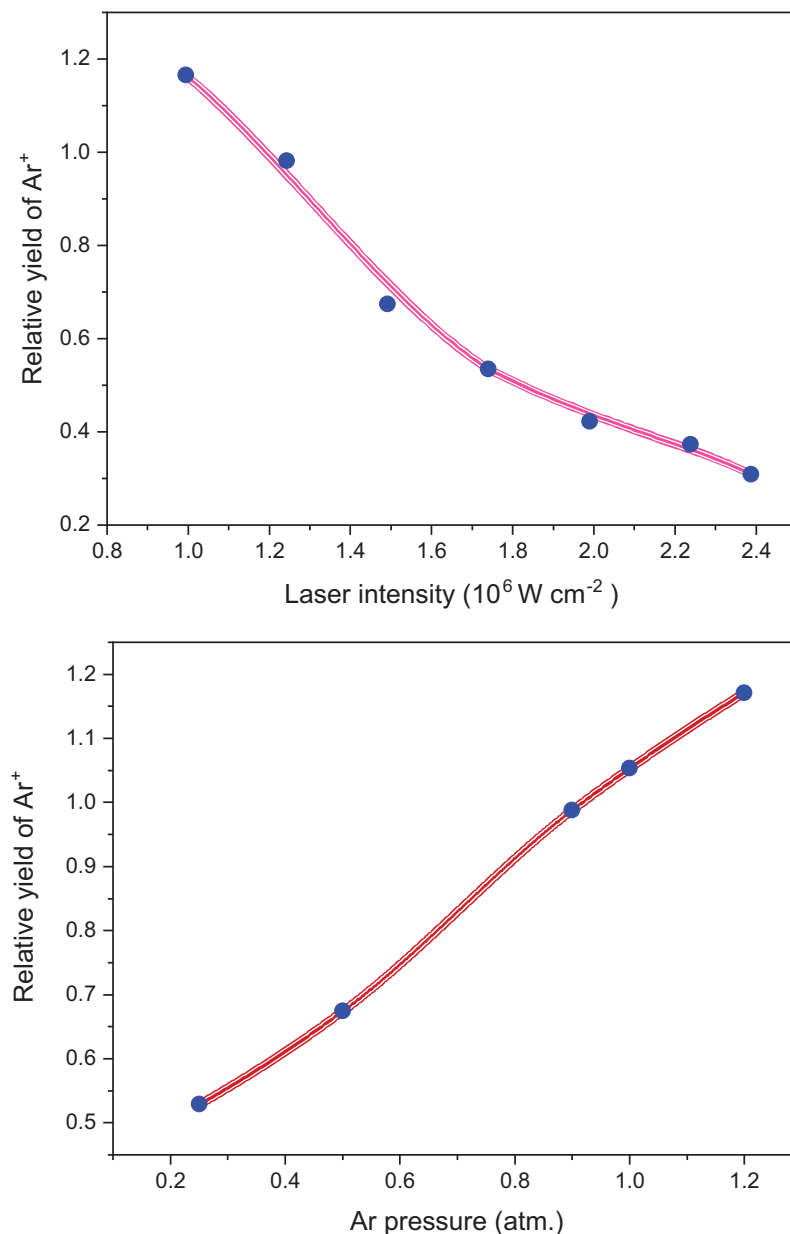


FIG. 4. **Relative yield of Ar⁺**: The ratio of the Ar⁺ yield to the total yield of all the other cations originating from photoexcited pyridine monomers is displayed. In the upper panel the laser intensity is varied and the argon pressure is fixed at 0.5 atm. In the bottom panel, the argon pressure is varied for a fixed laser intensity of $1.49 \times 10^6 \text{ Wcm}^{-2}$. For the details on the partial pressure of pyridine monomers, see the *Methods* section. These two measurements show that it is possible to optimize the concerted energy transfer from the photoexcited pyridine to argon by reducing the intensity of the laser or by increasing the partial pressure of argon.

the isotropic ejection of slow electrons, and the laser-power dependence of the relative yield of Ar cations, unequivocally reveal concerted and nonlocal energy transfer from four photoexcited pyridine units to an Ar atom. This novel ICD channel, wherein π^* -excited molecules ionize their atomic environment via concerted and nonlocal energy transfer, has wide implications in several fields. For instance, an efficient molecular mechanism that transfers energy from multiple photoacceptors to a distinct reaction center characterizes all

chemical systems of energy synthesis in Nature, including light harvesting (LH) systems. But unlike conventional LH systems, where the energy transfer from a photoacceptor to its reaction center is limited to resonant condition set by the charge separated state of the reaction center, a reaction is possible at the reaction center via ICD without the limitation of a resonance condition. Furthermore, our finding that photoexcited π -molecules of a system flare of their excitation energy by ionizing a distinct neighbouring atom raises a fundamental biological question: Has a similar concerted nonlocal energy transfer mechanism evolved along with the chemical evolution of π -chromophore-rich macromolecules, such as DNA, to avoid the apparent consequences of multiple photoabsorption by their chromophores? The fact that life on Earth has evolved under the conditions of intense UV light validates the existence of such a protective bio-molecular mechanism. Clearly, the advent of ICD as a fundamental molecular mechanism deep into many frontiers of science is evidenced by our observation that π^* -excited molecules ionize a distinct reaction center.

METHODS

Experimental methods

Gas-phase pyridine was diluted in argon gas before letting it into the interaction chamber through a solenoidal pulsed valve. The gas line was evacuated to 3.6×10^{-2} mbar using a dry pump before letting pyridine into the gas line. For the measurements on the relative yield of Ar^+ , as discussed in Figure 4 of the manuscript, pyridine vapour was let into the evacuated gas line through a needle valve to obtain a gas line pressure of about 1.1×10^{-1} mbar. Pure Ar gas of various partial pressures ranging from 0.25 to 1.2 atm was added to the same gas line. The gas mixture was then pulsed into the interaction chamber at 10 Hz. Measurements were made with a chamber pressure of 1×10^{-5} mbar, while operating at the above mentioned repetition rate. Argon ionization was observed even at 5×10^{-6} mbar pressure in the interaction chamber. The base pressure was maintained around 8×10^{-8} mbar. For the measurements on the pressure dependence of the relative yield of Ar^+ , the laser intensity was maintained at $1.49 \times 10^6 \text{ Wcm}^{-2}$.

The aperture of the nozzle was of 0.8 mm diameter and there was no formation of pyridine clusters at the above mentioned operating conditions. Nearly 10 cm downstream the nozzle exit, the gas pulse was collided with an unfocussed 266 nm Nd: YAG laser beam, midway between the first two electrodes of a time-of-flight mass spectrometer (TOFMS)³¹. A pulsed high voltage was applied to the repeller plate of the TOFMS to drive the ions towards the detector. The repeller voltage pulse was applied after a delay of about one microsecond post the laser pulse. The data acquisition was triggered by the TOF extraction pulse and hence the MCP dark counts were completely timed out. For electron measurements, the pyridine-Ar mixture was pulsed between the first two electrodes of a velocity-map imaging spectrometer²⁶ and the gas pulse was collided with 266 nm laser beam. The VMI spectrometer was carefully calibrated by performing photodetachment of anions with known electron affinities.

When the partial pressure of pyridine behind the nozzle is 10 mbar, it corresponds to a number density of $2.4 \times 10^{17} \text{ cm}^{-3}$. The interaction region is 125 nozzle diameters away from the nozzle. The density at the central line of the interaction region is thus about $2.4 \times 10^{13} \text{ cm}^{-3}$. Laser beam intersects the neutral beam at right angles. The number of photons in a 7 mJ (avg energy of the range of pulse energies employed) pulse of 266 nm beam = 9.3×10^{15} . The pyridine number density would vary as we move away from central beam, so considering an overlap cylinder of diameter 5 mm and length 5mm. Overlap volume is thus = 0.0981 cm^{-3} . The total number of molecules in this volume is 2.355×10^{12} . The photoabsorption cross-section at 266 nm, $\sigma = 19.3 \times 10^{-19} \text{ cm}^2$. $\sigma \times \text{target density} \times \text{photon flux} = 4.3 \times 10^{11} \text{ cm}^{-1}$ per pulse. The number of photoexcited pyridine molecules in the overlap volume = $4.3 \times 10^{11} \text{ cm}^{-1} \times 0.5 \text{ cm}$ per pulse = 2.15×10^{11} per pulse. Hence, in the interaction volume $V = 0.0981 \text{ cm}^{-3}$, the number of photoexcited pyridine is 2.15×10^{11} per pulse and the number of Ar atoms (partial pressure = 0.5 atm) present in the same volume $\approx 1 \times 10^{14}$. We detect about three to four Ar^+ cations per laser shot. ICD, being a long-range non-collisional process⁴, does not come under the realm of hard-sphere collision model. Calculation of ICD rates in the present case should take into account the attractive interactions between the dimers along with the initial and final states of the dimers.

Computational methods

Computation of the electronic structure of a molecular system consisting of four excited pyridine moieties and one argon atom using currently available bound state-based quantum chemical codes is a challenge. This is because the electronic state of the system containing four excited pyridines is above the ionization threshold when intermolecular interactions are active. Available quantum chemical methods are inadequate to account for such a state interacting with the ionization continuum. To overcome this difficulty, we used a

real-valued continuum remover potential based stabilization method²⁷. The real-valued continuum remover potential, applied at the non-interacting asymptote of the molecular potential, removes the discretized continuum descriptions of the fourfold excited state and transforms it into a bound state of the modified Hamiltonian.

In order to show the extent of covalent interaction in the excited state, the electron density in the stabilized excited state was calculated at the *excited-state Hartree-Fock* level²⁸. This calculation was performed using an in-house modified Gamess-US quantum chemical package^{27,29}. We imposed the symmetry of the orbitals as a constraint on the construction of the excited state density at each iteration step of the *excited-state Hartree-Fock* calculation. Since the intermolecular covalent interaction between π^* orbitals of pyridines is maximum when they cofacially approach, such geometric structures were chosen to measure the extent of inter-molecular covalent interaction. The molecular geometry of pyridine reported in Ref. 30 is used for the pyridine moieties. An atom centered 6-311 split valence Gaussian basis set, which is further augmented with three diffused even tempered Gaussians for the non-hydrogen atoms, is used in the calculation.

Acknowledgements

This work was supported by the Department of Science and Technology through project no: EMR/2016/005247 (G.A.).

Author contribution

S.B., G.A. and Y.S. conceived the concerted ICD. S.B. and G.A. planned the experiment and carried out the measurements with the support of N.R.B. and S.D. Y.S. planned the quantum-chemistry calculations. The results were discussed among the authors. Y.S. and G.A. wrote the manuscript.

Additional Information

Electronic supplementary information is available online for:

1. Kinetic energy spectrum of the emitted electrons.
2. Additional details on the experiment.
3. Absence of electron-impact ionization of argon in the present experiments.

Corresponding authors

Correspondence and request for materials should be addressed to G.A (garavind@iitm.ac.in) or Y.S. (sajeevy@barc.gov.in).

III. SUPPLEMENTARY MATERIAL

KINETIC ENERGY SPECTRUM OF THE EMITTED ELECTRONS.

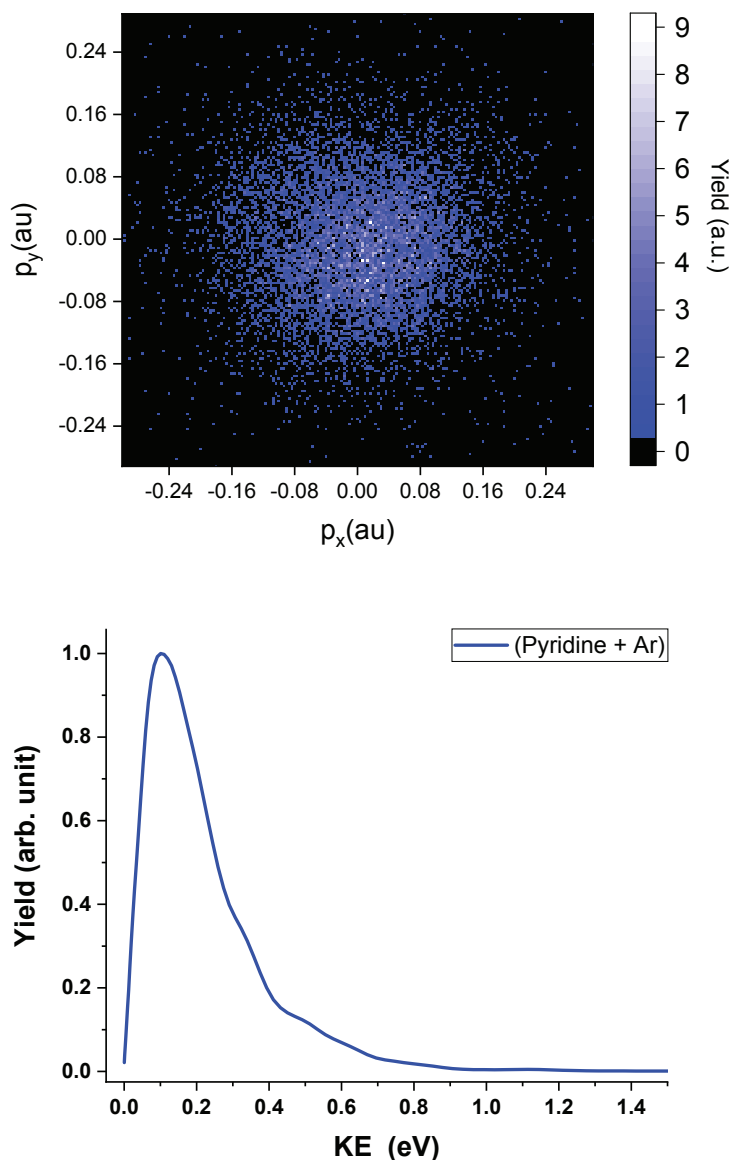


FIG. 5. Velocity Map Imaging (VMI) of electrons: The top panel displays the VMI of the electrons emitted and the bottom panel displays the kinetic energy of the released electrons. au, atomic units. a.u., arbitrary units.

Figure 5 shows the velocity map image of the ICD electrons with low kinetic energies. In most of the ICD experiments reported so far, excitation of one sub-unit of a dimer is the first step. Then an ultra-fast energy transfer from the excited sub-unit to the other sub-unit of the dimer ionizes the latter. In such cases, the maximum kinetic energy of the ejected electrons will be the difference between the excitation energy in the dimer and the ionization energy. However, in the present experiment, since the initial excitation is in unbound molecular monomers, we expect slow ICD electrons, as discussed below.

On photoexcitation of pyridine monomers, Intramolecular vibrational redistribution (IVR) leads to transfer of the excess electronic energy into the nuclear modes. When ICD occurs *en route* to the association of these excited monomers, only a small fraction of energy in the nuclear modes becomes available for ICD ionization leading to slow electrons. This is because ICD occurs faster than the relaxation of energy from the nuclear modes back to the electronic mode. Since IVR is the characteristic of the photoabsorbing π -molecules, the range of kinetic energy for the ICD electrons should not differ much for the ICD ionization of pyridine molecules³¹ and Ar atoms. Further, the observed isotropic emission of the ICD electrons is characteristic of ICD ionization.

ADDITIONAL DETAILS ON THE EXPERIMENT

Electron measurements: The VMI electrodes were plated with gold, whose workfunction is above the photon energy (4.661 eV).

Ion measurements: The photon energy is above the workfunction of the stainless steel TOFMS electrodes (≈ 4.4 eV). In order to avoid the acceleration of the photoelectrons, if any, produced from the surfaces of the TOFMS electrodes, we had applied the TOFMS pulsed electric-field with a finite time-delay *after* the laser-pulse. As mentioned in the *Methods* section, this delay was about 1 microsecond, which is sufficient to get rid of the photoelectrons (≈ 0.26 eV) from the volume contained by the TOFMS electrodes. We did not apply an electric-field exclusively to sweep photoelectrons produced, if any. We had also performed SIMION simulations, which show that even if photoelectrons were produced from the TOF electrode surfaces and are accelerated, their path would result in the formation of Ar^+ *much* away from the central volume of the first two TOF plates. In such a situation we see that the field is unable to manoeuvre the ions to the detector, which is located 1 meter away from the interaction region. TOF electric field is optimized to collect ions produced at the overlap of laser-gas beam region. Ions produced at random locations will also result in a very broad TOF peak, which is also not seen for any of our ions. Thus, with great care we have ensured the absence of any role of photoelectrons.

Thus Ar^+ were not formed on irradiation of *pure-Ar gas alone*, as shown in the Figure 6 (blue points). We observe Ar^+ only when *pyridine-Ar gas mixture* is irradiated and most importantly, the Ar^+ yield depends on the density of the pyridine gas, as seen by comparing the black and red data points in the Figure 6. The latter clearly asserts that the ionization of Ar is due to concerted energy-transfer from photoexcited pyridine molecules. Note that the yield in Figure 6 decreases with increasing time-delay. This is due to the degrading collection efficiency as the initial position of the ions deviate from the volume centered between the first two TOFMS electrodes.

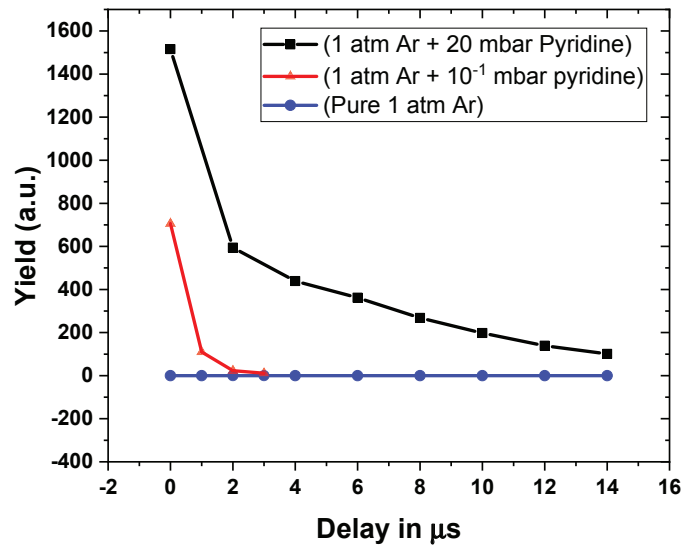


FIG. 6. The yield of Ar^+ cations as a function of the delay between the laser pulse and the TOFMS electric-field pulse. The laser energy was maintained the same for these data points.

ABSENCE OF ELECTRON-IMPACT IONIZATION OF ARGON IN THE PRESENT EXPERIMENTS

We describe below our experiments to that rule out electron-impact ionization of argon in our experiments. Figure 7 shows the schematic of our time-of-flight spectrometer (TOF) along with the voltages applied. The distance between adjacent electrodes = 2 cm.

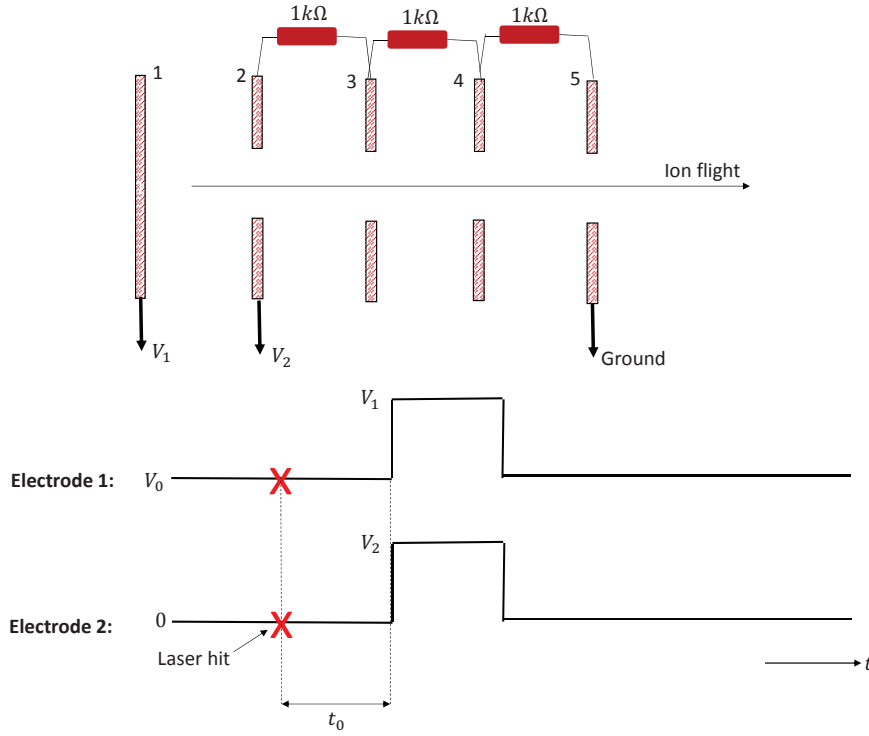


FIG. 7. *Electrode 1*: A pulsed voltage V_1 is applied over a DC base voltage V_0 . *Electrode 2*: A pulsed voltage V_2 is applied w.r.t. to the ground. The ions and electrons formed between the first two electrodes experience a DC electric field of $50V_0$ V/m for t_0 microseconds, before the application of the high voltage pulses that drive the cations towards the detector.

For a DC potential difference of V_0 between the first two electrodes, the acceleration for an electron is

$$a = \frac{Eq}{m_e} = \frac{50V_0 * q}{m_e} = 8.8V_0 \times 10^{12} \text{ m/s}^2$$

When $V_0 = 0.5V$:

(a) The time taken by an electron produced at the center of the interaction region, with zero KE, to hit the first TOF electrode is

$$t = \sqrt{\frac{2 \times 0.01m}{4.4 \times 10^{12}m/s^2}} = 67 \text{ ns}$$

(b) An electron produced with 0.2 eV and with an initial velocity directed away from the first TOF electrode will travel 8 mm before it turns around. The total time for it to hit the first TOF electrode is

$$t = \left(\frac{1}{a} \times \sqrt{\frac{2 \times 0.2eV}{m_e}} \right) + \sqrt{\frac{2 \times 18mm}{a}} \approx 150ns$$

Therefore for $V_0 = 0.5V$ and a delay of $1 \mu s$ between the laser-hit and the high-voltage extraction, there won't be any electrons present in the interaction region when the high-voltage pulse arrives!

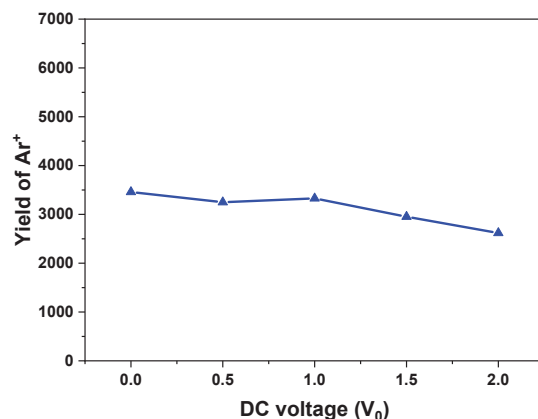


FIG. 8. The yield of Ar^+ cations as a function of V_0 , the DC voltage that sweeps the electrons.

Figure 8 shows that the yield of Ar^+ is nearly the same with and without the application of the electron sweeping voltage V_0 . For different V_0 values, the initial positions and energies of the Ar^+ cations prior to the application of the high-voltage pulse differ, resulting in slight variation in the efficiency of their collection at the detector, which is situated one meter away from the interaction point. This reflects in the minor variation in the Ar^+ yield as V_0 changes. Thus, there is no contribution of ICD electrons in ionizing the Argon atoms.

Earth's magnetic field: Since the above experiments reveal the absence of any electron during the arrival of the high-voltage pulse, the Earth's magnetic field does not also have a role here.

Additional experiment

We also performed an additional experiment, wherein $V_0 = 0$ but the potential difference

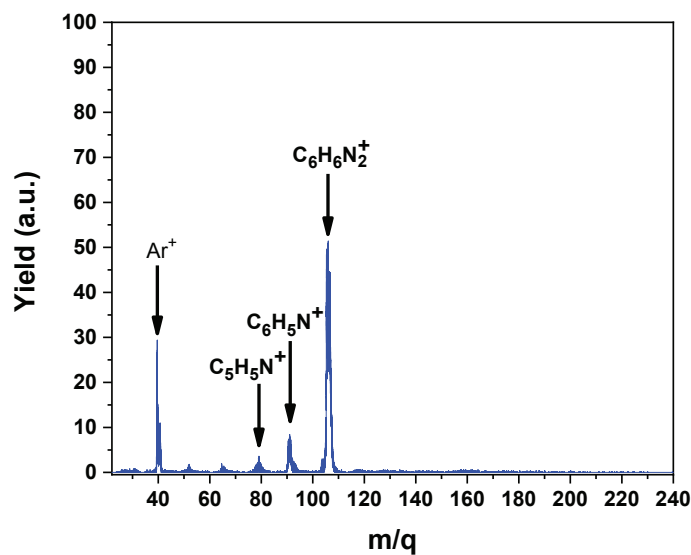


FIG. 9. Mass spectra obtained by applying $V_1 = 402V$ and $V_2 = 392V$. Laser and gas-beam conditions are the same. No electron sweeping potential is applied.

between the first two electrodes was maintained at 10 Volts! $V_1 = 402V$ and $V_2 = 392V$. Thus the maximum energy gained by any electron is 10 eV, which is insufficient to ionize

Argon (I.P. = 15.6 eV). Figure 9 shows that the mass spectra thus obtained is the same as the mass spectra obtained in our original experiments (Figure 1 of the main manuscript). Thus, there is no electron-impact ionization of Argon in our experiments.

(a) In fact, the kinetic energy of the ICD electrons from pyridine peaks at 80 meV, corresponding to a velocity of 1.7×10^5 m/s. Hence the ICD electrons will move away from the interaction region (2 cm wide) in 0.1 μ s. Therefore these electrons will not be present when the high-voltage pulse arrives 1 μ s post laser-hit, as done in our original experiments.

(b) Moreover, collisional ionization of Ar by the ICD electrons from pyridine, being a secondary process, should result in a very low yield of Ar^+ relative to the pyridine cations. On the contrary, as shown in Fig 4 of the main manuscript, with *decreasing* laser intensity, the relative yield $[\text{Ar}^+] / [\text{pyridine cations}]$ tends to 1!

Points (a), (b), the results of the weak DC-electric field experiment and the additional experiment described above, together with the observed variation of the relative yield $[\text{Ar}^+] / [\text{pyridine cations}]$ with the laser intensity, unambiguously assert the concerted ICD ionization of Ar in our experiments.

Ion-TOF spectra with no gas and with only Argon gas

We also present the ion-TOF spectra for (a) no gas (background) and (b) only argon gas. There is no Ar^+ signal seen, when only pure argon gas is irradiated with 266nm. These two spectra were taken even without a delay in the extraction pulse w.r.t to the laser pulse. These spectra also assert that there is no formation of Ar^+ due to impact with accelerated photoelectrons. These data were taken with the laser intensity and data collection time same as that for Fig 1 of the manuscript and hence the yields could be compared with each other. Only a very weak background ion signal is seen.

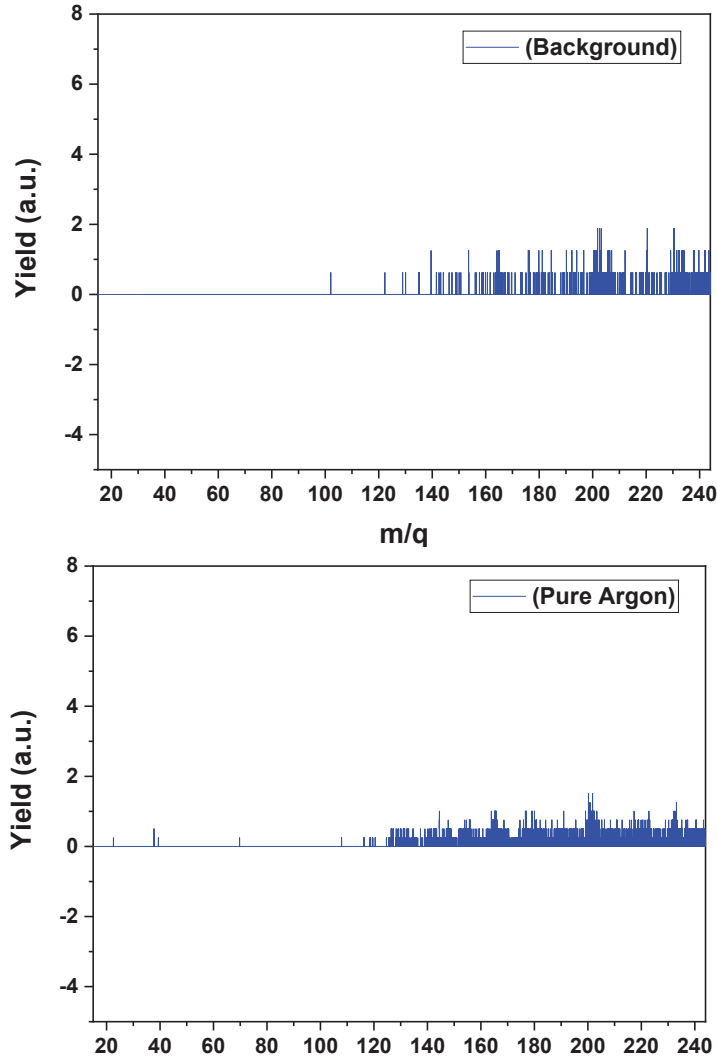


FIG. 10. Ion TOF spectra for the background and pure Argon gas are presented. These data were taken with the laser intensity and data collection time same as that for Fig 1 of the manuscript.

Electron spectra with no gas and with only Argon gas

The spectra Fig. 11 and Fig. 12 are the electron spectra obtained for (a) no gas and (b) argon only, respectively. The data were taken for 10000 laser shots with the same laser intensity as employed in Fig 2 of the manuscript. A structureless weak background electron signal is seen for both the spectra with equal counts! This unambiguously rules out Ar^+ signal when only Argon is irradiated with 266nm.

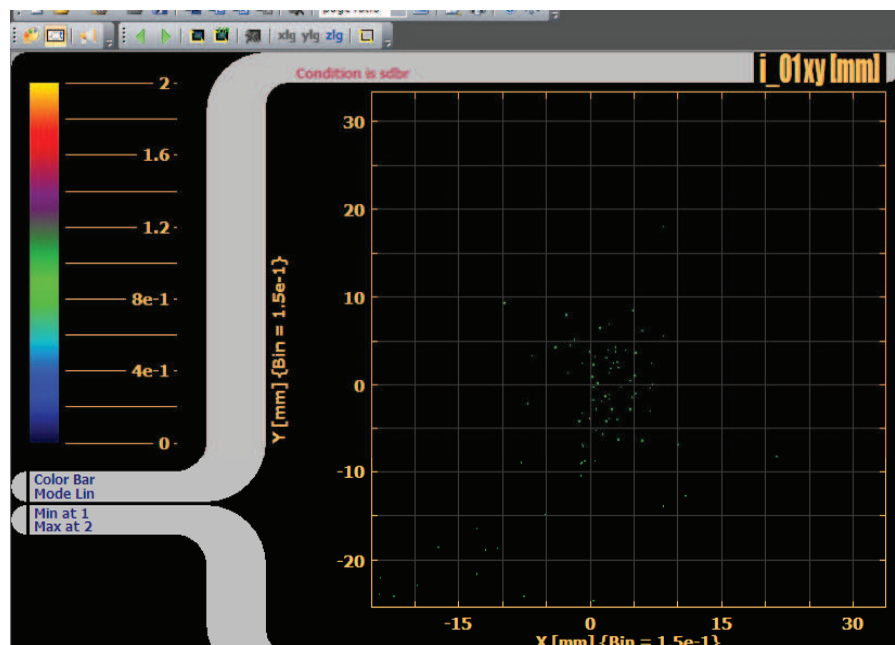


FIG. 11. Electron VMI with no gas. The data is taken for 10000 laser shots with intensity same as employed for Fig 2. of our manuscript. This weak structureless spectra has count equal to 85.

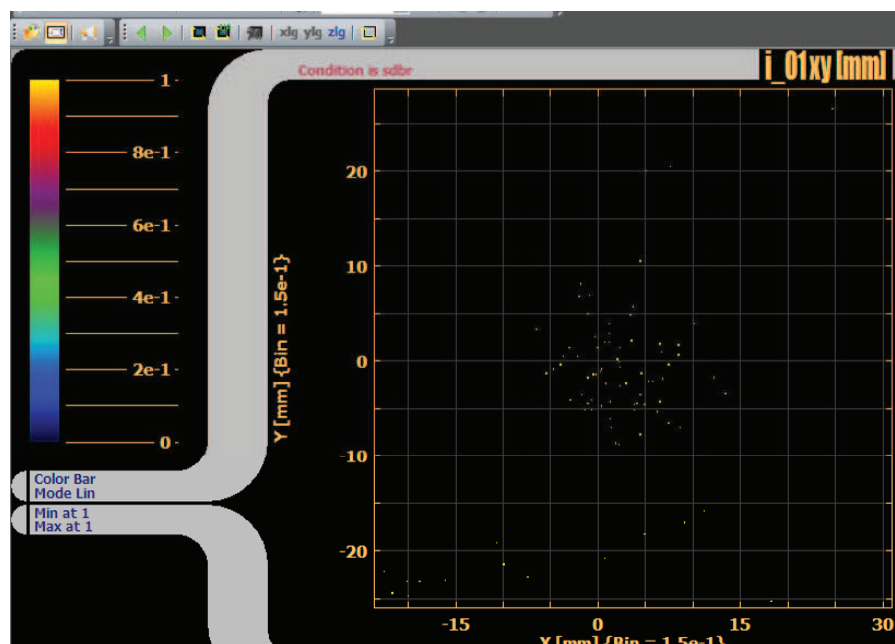


FIG. 12. Electron VMI with only argon gas. The data is taken for 10000 laser shots with intensity same as employed for Fig 2. of our manuscript. This weak structureless spectra has count equal to 84.

- ¹L. S. Cederbaum, J. Zobeley, and F. Tarantelli, Giant intermolecular decay and fragmentation of clusters, *Phys. Rev. Lett.* **79**, 4778 (1997).
- ²A. I. Kuleff, K. Gokhberg, S. Kopelke, and L. S. Cederbaum, Ultrafast interatomic electronic decay in multiply excited clusters, *Phys. Rev. Lett.* **105**, 043004 (2010).
- ³P. V. Demekhin, K. Gokhberg, G. Jabbari, S. Kopelke, A. I. Kuleff, and L. S. Cederbaum, Overcoming blockade in producing doubly excited dimers by a single intense pulse and their decay, *J. Phys. B: At. Mol. Opt. Phys.* **46**, 021001 (2013).
- ⁴T. Jahnke, U. Hergenbahn, B. Winter, R. Dörner, U. Fröhling, P. V. Demekhin, K. Gokhberg, L. S. Cederbaum, A. Ehresmann, A. Knie, and A. Dreuw, Interatomic and intermolecular coulombic decay, *Chem. Rev.* **120**, 11295 (2020).
- ⁵T. Jahnke, Interatomic and intermolecular coulombic decay: the coming of age story, *J. Phys. B: At. Mol. Opt. Phys.* **48**, 082001 (2015).
- ⁶X. Ren, J. Zhou, E. Wang, T. Yang, Z. Xu, N. Sisourat, T. Pfeifer, and A. Dorn, Ultrafast energy transfer between π -stacked aromatic rings upon inner-valence ionization, *Nat. Chem.* **14**, 232–238 (2022).
- ⁷T. Jahnke, H. Sann, T. Havermeier, K. Kreidi, C. Stuck, M. Meckel, M. Schöffler, N. Neumann, R. Wallauer, S. Voss, *et al.*, Ultrafast energy transfer between water molecules, *Nature Phys* **6**, 139 (2010).
- ⁸D. Buchta, S. R. Krishnan, N. B. Brauer, M. Drabbels, P. O’Keeffe, M. Devetta, M. Di Fraia, C. Callegari, R. Richter, M. Coreno, K. C. Prince, F. Stienkemeier, R. Moshhammer, and M. Mudrich, Charge transfer and penning ionization of dopants in or on helium nanodroplets exposed to euv radiation, *J. Phys. Chem. A* **117**, 4394 (2013).
- ⁹C. Richter, D. Hollas, C.-M. Saak, M. Förstel, T. Miteva, M. Mucke, O. Björneholm, N. Sisourat, P. Slavíček, and U. Hergenbahn, Competition between proton transfer and intermolecular coulombic decay in water, *Nat Commun* **9**, 1 (2018).
- ¹⁰A. LaForge, M. Drabbels, N. B. Brauer, M. Coreno, M. Devetta, M. Di Fraia, P. Finetti, C. Grazioli, R. Katzy, V. Lyamayev, *et al.*, Collective autoionization in multiply-excited systems: a novel ionization process observed in helium nanodroplets, *Scientific reports* **4**, 1 (2014).
- ¹¹K. Nagaya, D. Iablonskyi, N. Golubev, K. Matsunami, H. Fukuzawa, K. Motomura, T. Nishiyama, T. Sakai, T. Tachibana, S. Mondal, *et al.*, Interatomic coulombic decay cascades in multiply excited neon clusters, *Nat Commun* **7**, 1 (2016).
- ¹²A. Dubrouil, M. Reduzzi, M. Devetta, C. Feng, J. Hummert, P. Finetti, O. Plekan, C. Grazioli, M. D. Fraia, V. Lyamayev, A. L. Forge, R. Katzy, F. Stienkemeier, Y. Ovcharenko, M. Coreno, N. Berrah, K. Motomura, S. Mondal, K. Ueda, K. C. Prince, C. Callegari, A. I. Kuleff, P. V. Demekhin, and G. Sansone, Two-photon resonant excitation of interatomic coulombic decay in neon dimers, *J. Phys. B: At. Mol. Opt. Phys.* **48**, 204005 (2015).
- ¹³N. Sisourat, N. V. Kryzhevoi, P. Kolorenč, S. Scheit, T. Jahnke, and L. S. Cederbaum, Ultralong-range en-

- ergy transfer by interatomic coulombic decay in an extreme quantum system, *Nature Phys* **6**, 508 (2010).
- ¹⁴K. Gokhberg, P. Kolorenč, A. I. Kuleff, and L. S. Cederbaum, Site-and energy-selective slow-electron production through intermolecular coulombic decay, *Nature* **505**, 661 (2014).
- ¹⁵T. Havermeier, T. Jahnke, K. Kreidi, R. Wallauer, S. Voss, M. Schöffler, S. Schössler, L. Foucar, N. Neumann, J. Titze, H. Sann, M. Kühnel, J. Voigtsberger, J. H. Morilla, W. Schöllkopf, H. Schmidt-Böcking, R. E. Grisenti, and R. Dörner, Interatomic coulombic decay following photoionization of the helium dimer: Observation of vibrational structure, *Phys. Rev. Lett.* **104**, 133401 (2010).
- ¹⁶R. Cabrera-Trujillo, O. Vendrell, and L. S. Cederbaum, Interatomic coulombic decay of a li dimer in a coupled electron and nuclear dynamics approach, *Phys. Rev. A* **102**, 032820 (2020).
- ¹⁷A. LaForge, M. Shcherbinin, F. Stienkemeier, R. Richter, R. Moshhammer, T. Pfeifer, and M. Mürdrich, Highly efficient double ionization of mixed alkali dimers by intermolecular coulombic decay, *Nature Phys* **15**, 247 (2019).
- ¹⁸Y. Kumagai, H. Fukuzawa, K. Motomura, D. Iablonskyi, K. Nagaya, S.-i. Wada, Y. Ito, T. Takanashi, Y. Sakakibara, D. You, T. Nishiyama, K. Asa, Y. Sato, T. Umemoto, K. Kariyazono, E. Kukk, K. Kooser, C. Nicolas, C. Miron, T. Asavei, L. Neagu, M. S. Schöffler, G. Kastirke, X.-j. Liu, S. Owada, T. Katayama, T. Togashi, K. Tono, M. Yabashi, N. V. Golubev, K. Gokhberg, L. S. Cederbaum, A. I. Kuleff, and K. Ueda, Following the birth of a nanoplasma produced by an ultrashort hard-x-ray laser in xenon clusters, *Phys. Rev. X* **8**, 031034 (2018).
- ¹⁹P. Zhang, C. Perry, T. T. Luu, D. Matselyukh, and H. J. Wörner, Intermolecular coulombic decay in liquid water, *Phys. Rev. Lett.* **128**, 133001 (2022).
- ²⁰J. Zhou, X. Yu, S. Luo, X. Xue, S. Jia, X. Zhang, Y. Zhao, X. Hao, L. He, C. Wang, D. Ding, and X. Ren, Triple ionization and fragmentation of benzene trimers following ultrafast intermolecular Coulombic decay, *Nat Commun* **13**, 5335 (2022).
- ²¹S. Barik, S. Dutta, N. R. Behera, R. K. Kushawaha, Y. Sajeev, and G. Aravind, Ambient-light-induced intermolecular Coulombic decay in unbound pyridine monomers, *Nat. Chem.* **14**, 1098 (2022).
- ²²C. Crespo-Hernández, K. de La Harpe, and B. Kohler, Ground-state recovery following uv excitation is much slower in g-c dna duplexes and hairpins than in mononucleotides, *Journal of the American Chemical Society* **130**, 10844 (2008).
- ²³E. Brun, P. Cloutier, C. Sicard-Roselli, M. Fromm, and L. Sanche, Damage induced to dna by low-energy (0–30 eV) electrons under vacuum and atmospheric conditions, *J. Phys. Chem. B* **113**, 10008 (2009).
- ²⁴I. Bald, J. Kopyra, I. Dabkowska, E. Antonsson, and E. Illenberger, Low energy electron-induced reactions in gas phase 1,2,3,5-tetra-o-acetyl- β -d-ribofuranose: A model system for the behavior of sugar in dna, *J. Chem. Phys.* **126**, 074308 (2007).
- ²⁵F. Martin, P. D. Burrow, Z. Cai, P. Cloutier, D. Hunting, and L. Sanche, Dna strand breaks induced by 0–4 eV electrons: The role of shape resonances, *Phys. Rev. Lett.* **93**, 068101 (2004).
- ²⁶S. Barik, A. K. Kanakati, S. Dutta, N. R. Behera, R. K. Kushawaha, and G. Aravind, Low-lying dipole resonances in fecn: A viable formation pathway for fecn in space, *The Astrophysical Journal* **931**, 47 (2022).
- ²⁷Y. Sajeev, Real-valued continuum remover potential: An improved L^2 -stabilization method for the chemistry of electronic resonance states, *Chem. Phys. Lett.* **587**, 105 (2013).
- ²⁸Y. Sajeev, Eomcc over excited state hartree-fock solutions (eshf-eomcc): An efficient approach for the entire ground state potential energy curves of higher-order bonds, *AIP Advances* **5**, 087140 (2015).
- ²⁹G. M. J. Barca, C. Bertoni, L. Carrington, D. Datta, N. De Silva, J. E. Deustua, D. G. Fedorov, J. R. Gour, A. O. Gunina, E. Guidez, T. Harville, S. Irle, J. Ivanic, K. Kowalski, S. S. Leang, H. Li, W. Li, J. J. Lutz, I. Magoulas, J. Mato, V. Mironov, H. Nakata, B. Q. Pham, P. Piecuch, D. Poole, S. R. Pruitt, A. P. Rendell, L. B. Roskop, K. Ruedenberg, T. Sattasathuchana, M. W. Schmidt, J. Shen, L. Slipchenko, M. Sosonkina, V. Sundriyal, A. Tiwari, J. L. Galvez Vallejo, B. Westheimer, M. Włoch, P. Xu, F. Zahariev, and M. S. Gordon, Recent developments in the general atomic and molecular electronic structure system, *J. Chem. Phys.* **152**, 154102 (2020).
- ³⁰Z.-L. Cai and J. R. Reimers, The low-lying excited states of pyridine, *J. Phys. Chem. A* **104**, 8389 (2000).
- ³¹Barik, S. *et al.* Ambient-light-induced intermolecular Coulombic decay in unbound pyridine monomers. *Nat. Chem.* **14**, 1098–1102 (2022).
<https://doi.org/doi.org/10.1038/s41557-022-01002-2>

Clip A Frame

Clip B Frame